

DEEP NEURAL NETWORKS FOR SOLVING EXTREMELY LARGE LINEAR SYSTEMS

YIQI GU* AND MICHAEL K. NG*

Abstract. In this paper, we study deep neural networks for solving extremely large linear systems arising from physically relevant problems. Because of the curse of dimensionality, it is expensive to store both solution and right-hand side vectors in such extremely large linear systems. Our idea is to employ a neural network to characterize the solution with parameters being much fewer than the size of the solution. We present an error analysis of the proposed method provided that the solution vector can be approximated by the continuous quantity, which is in the Barron space. Several numerical examples arising from partial differential equations, queueing problems and probabilistic Boolean networks are presented to demonstrate that solutions of linear systems with sizes ranging from septillion (10^{24}) to nonillion (10^{30}) can be learned quite accurately.

Key words. very large-scale linear systems; neural networks; Riesz fractional diffusion; overflow queueing model; probabilistic Boolean networks;

AMS subject classifications. 65F10; 65F50; 65N22; 68T07; 60K25

1. Introduction. Linear equations appear widely in applied problems such as partial differential equations and numerical optimization. In physically relevant problems, one usually needs to compute some physical quantity v such as temperature distribution and fluid velocity. Let us suppose the problem is addressed in a d -dimensional domain $\Omega \subset \mathbb{R}^d$, in which a grid Γ is set up. A grid function u on Γ is thereafter introduced to approximate v . Then after using special discretization on the problem, u is computed through the following system of linear equations,

$$(1.1) \quad \mathbf{A} \mathbf{u} = \mathbf{b},$$

where $\mathbf{A} \in \mathbb{R}^{\tilde{N} \times \tilde{N}}$ is a non-singular matrix; $\mathbf{b} \in \mathbb{R}^{\tilde{N}}$ is a given vector; $\mathbf{u} = \text{vec}(u) \in \mathbb{R}^{\tilde{N}}$ is the vector representation of u ; \tilde{N} is the degree of freedom.

1.1. Existing methods and difficulties. Traditional linear solvers, including direct and iterative methods, have been extensively studied for a long time. Despite high efficiency and accuracy for small-scale systems, they are inefficient for systems having very large sizes. One typical example lies in that Ω is a d -dimensional box and (1.1) is assembled with tensor product structure on a $N \times N \times \cdots \times N$ (d times) grid. A series of methods have been developed for the linear system with tensor product structure, such as Krylov subspace method [24], projection method [2], and Cayley transformation [18]. However, for such linear systems, the number of equations or unknowns $\tilde{N} = N^d$ that is extremely large even if d is moderately large. In spite of some development concerning large-scale problems [1, 45, 33], the practical performance of many existing methods is still limited by the dimension. For high-dimensional problems with larger d , the system size N^d might exceed the machine storage so that even the column vector \mathbf{u} or \mathbf{b} can not be saved entirely in memory.

1.2. Motivations and contributions. In recent years, the theory and applications of neural networks (NNs) have been widely studied in a variety of areas, including computer science

*Department of Mathematics, The University of Hong Kong, Pokfulam, Hong Kong (yiqigu@hku.hk, mng@maths.hku.hk). This work is supported by HKRGC GRF 12300218, 12300519, 17201020 and 17300021.

and applied mathematics. Generally speaking, NN is a type of function with a nonlinear parametric structure. It has been found in a series of literature that NNs can approximate common functions effectively. In the pioneering work [10, 20, 4], the universal approximation theory of two-layer shallow NNs is discussed. In recent research, quantitative information about the NN approximation error is discovered for various types of functions, e.g., smooth functions [29, 27, 42, 16, 31, 40, 14, 15], piecewise smooth functions [34], band-limited functions [32], continuous functions [43, 36, 37].

One remarkable property of NNs is the capability of high-dimensional approximation. Many traditional approximation structures such as finite element and polynomials suffer from the curse of dimensionality. Specifically, when approximating a function of d -dimensional variable, their error bounds will be $O(N^{-\alpha/d})$, where N is the number of free parameters and α characterizes the regularity of the function. However, NNs can avoid such issues for some special function spaces. A typical example is the Barron space, for which the NN approximation error is either independent of d or increasing with d very slowly [3, 4, 23, 17, 13, 38, 39, 6, 15]. So far, NNs have been applied successfully in solving high-dimensional differential equations and inverse problems [19, 35, 41, 44, 22].

In this work, we propose a novel method to solve linear system (1.1) using NNs. Note that in many real-world problems, the physical quantities are usually continuously distributed. The basic idea of our method comes from that if the physical quantity v is smooth enough in Ω , NNs with only a small number of parameters can approximate v with the desired accuracy. Meanwhile, if the true solution \mathbf{u} of (1.1) is a good approximation to v , it can be also accurately approximated by such NNs. This allows us to take a neural network ϕ to characterize \mathbf{u} with parameters much fewer than $\tilde{N} = N^d$. More precisely, the unknown numeric vector \mathbf{u} in (1.1) is replaced with an NN-based vector, whose parameters are to be computed instead. In the proposal, the new system is solved by a least-squares method under a deep learning framework. This approach is able to solve linear systems of very large sizes that may be difficult for existing methods. Error analysis is also conducted for this method provided that the true physical quantity is in the Barron space.

Several typical problems are solved using the proposed method in numerical experiments. The first problem is the structured linear system derived from Poisson's equation using the second-order finite difference scheme, in which the system with $(N, d) = (10^4, 6)$ is solved effectively. Next, we consider linear systems derived from Riesz fractional diffusion [21] and the overflow queuing problem [7, 8, 9], where we succeed in the implementation of 10 dimensions, while early work can at most address 3 dimensions numerically. Moreover, as the last example, we solve a $2^d \times 2^d$ sparse system from the probabilistic Boolean network problem. Our method is implemented successfully to solve the problem with 100 dimensions and $O(10^{30})$ nonzero entries, while previous work [26] merely addresses 30 dimensions and $O(10^4)$ nonzero entries.

1.3. Organization of paper. This paper is organized as follows. In Section 2, we review the fully-connected neural networks, the conceptual NN-based method, and the practical algorithms with gradient descent. In Section 3, we estimate the error of the approximate solution under the Barron space hypothesis. Several physically relevant examples are demonstrated in Section 4 to test the performance of the proposed method. Conclusions and discussions about further research work are provided in Section 5.

2. NN-based Method.

2.1. Fully-connected neural network. Among the many types of neural networks, the fully connected neural network (FNN) is the most basic and commonly used in applied mathematics.

Mathematically speaking, given $L \in \mathbb{N}^+$ and $M_\ell \in \mathbb{N}^+$ for $\ell = 0, 1, \dots, L-1$, we define the simple nonlinear function $h_\ell : \mathbb{R}^{M_{\ell-1}} \rightarrow \mathbb{R}^{M_\ell}$ given by

$$(2.1) \quad h_\ell(x_\ell) := \sigma(W_\ell x_\ell + b_\ell)$$

where $W_\ell \in \mathbb{R}^{M_\ell \times M_{\ell-1}}$; $b_\ell \in \mathbb{R}^{M_\ell}$; $\sigma(x)$ is a given function which is applied entry-wise to a vector x to obtain another vector of the same size, named activation function. Common activation functions include rectified linear unit (ReLU) $\max\{0, x\}$ and the sigmoidal function $(1 + e^{-x})^{-1}$.

Set $M_0 = d$, the dimension of the input variable, then an FNN $\phi : \mathbb{R}^d \rightarrow \mathbb{R}$ is formulated as the composition of these $L-1$ simple nonlinear functions, namely

$$(2.2) \quad \phi(x; \theta) = a^\top h_{L-1} \circ h_{L-2} \circ \dots \circ h_1(x) \quad \text{for } x \in \mathbb{R}^d,$$

where $a \in \mathbb{R}^{M_{L-1}}$ and $\theta := \{a, W_\ell, b_\ell : 1 \leq \ell \leq L-1\}$ denotes the set of all free parameters. Here M_ℓ is named as the width of the ℓ -th layer and L is named as the depth. If fixing σ , L and $\{M_\ell\}_{\ell=1}^{L-1}$, the FNN architecture is completely determined. In the following passage, for simplicity, we only consider the architecture with fixed width $M_\ell = M$ for all $\ell = 1, \dots, L-1$. We use $\mathcal{F}_{L,M,\sigma}$ to denote the set of all FNNs with depth L , width M and activation function σ .

2.2. A conceptual method. We will conceptually introduce the FNN-based method for the linear system (1.1). As a typical example, we consider that the original physical domain Ω is a d -dimensional unit box, and a Cartesian grid is set up on it. This method can be easily generalized for other domain geometries and grid settings.

Specifically, let $\Omega = [0, 1]^d$, $N \in \mathbb{N}^+$ and $0 \leq x_1 < \dots < x_N \leq 1$, then

$$(2.3) \quad \Gamma = \{(x_{i_1}, \dots, x_{i_d})\}_{i_1, \dots, i_d=1}^N$$

forms a set of grid points in Ω . In many applications, one uses a d -way array \mathbf{u} , which is lexicographically ordered as

$$(2.4) \quad \mathbf{u} = [u_{1,1,\dots,1} \ u_{1,1,\dots,2} \ \dots \ u_{N,N,\dots,N}]^\top \in \mathbb{R}^{N^d},$$

to approximate a physical function v on Γ by the following relation

$$(2.5) \quad u_{i_1, \dots, i_d} \approx v(x_{i_1}, \dots, x_{i_d}), \quad \forall (x_{i_1}, \dots, x_{i_d}) \in \Gamma.$$

If the original problem is discretized by special schemes, a system of linear equations for \mathbf{u} can be derived, say

$$(2.6) \quad \mathbf{A}\mathbf{u} = \mathbf{b},$$

where $\mathbf{A} \in \mathbb{R}^{N^d \times N^d}$ is the matrix corresponding to the discretization and $\mathbf{b} \in \mathbb{R}^{N^d}$ is a vector given by the problem.

In most cases, the number of grid points N in every dimension should be set large to obtain high accuracy of the discretization. Therefore one difficulty of solving (2.6) lies in the case when d is moderately large (e.g., $d \geq 10$). At the very worst, N^d exceeds the total storage, and even a vector in \mathbb{R}^{N^d} can not be saved entirely in memory.

Fortunately, in many situations, the physical function v is smooth and continuously varying in Ω . Since NNs have the capability of approximating high-dimensional smooth functions, there exist

FNNs that are close to v . We also note that \mathbf{u} is supposed to be a good approximation to v on Γ . So it is natural to connect \mathbf{u} with certain FNNs. Following this idea, we propose to use an FNN $\phi \in \mathcal{F}_{L,M,\sigma}$ to represent \mathbf{u} approximately; namely, we let

$$(2.7) \quad \phi(x_{i_1}, \dots, x_{i_d}; \theta) \approx u_{i_1, \dots, i_d}, \quad \forall (x_{i_1}, \dots, x_{i_d}) \in \Gamma,$$

or in vector form,

$$(2.8) \quad \Phi(\theta) := [\phi(x_1, \dots, x_1; \theta) \ \phi(x_1, \dots, x_2; \theta) \ \cdots \ \phi(x_N, \dots, x_N; \theta)]^\top \approx \mathbf{u}.$$

Note that the number of parameters $|\theta| = (L-2)M^2 + (L+d)M$, which could be much smaller than N^d in the practical implementation (see Section 4 for numerical examples). So (2.8) provides a representation of \mathbf{u} with much less storage. It allows us to deal with systems of very large sizes. Similar to (2.6), we can derive a system for Φ ,

$$(2.9) \quad \mathbf{A}\Phi = \mathbf{b}.$$

We have two comments about the system (2.9). First, due to the nonlinear structure of ϕ , (2.9) is a system of nonlinear equations with unknown θ . Second, since the number of unknowns $|\theta|$ is supposed to be smaller than the number of equations N^d , one usually can not find an exact solution. Instead, we will find the least-squares solution through the following optimization,

$$(2.10) \quad \min_{\theta} L(\theta) := \frac{1}{N^d} \|\mathbf{A}\Phi(\theta) - \mathbf{b}\|_2^2.$$

The loss function L can be reduced via gradient descent methods under the deep learning framework. If a feasible solution θ_0 is found, the error between $\Phi(\theta_0)$ and the true solution \mathbf{u} of (2.6) is estimated by

$$(2.11) \quad \|\Phi(\theta_0) - \mathbf{u}\|_2 \leq \|\mathbf{A}^{-1}\|_2 \|\mathbf{A}(\Phi(\theta_0) - \mathbf{u})\|_2 \leq \|\mathbf{A}^{-1}\|_2 \sqrt{N^d L(\theta_0)}.$$

Therefore the above method finds an approximate solution with the error bounded by the condition number of the matrix and the final minimized loss.

2.3. Non-unique solutions. If the linear system has more than one solution, the optimization (2.10) may not locate the particular solution we are looking for. One typical problem is the computation of the nontrivial solutions of homogeneous systems. For example, the eigenvectors of \mathbf{A} can be computed through $(\lambda \mathbf{I} - \mathbf{A})\mathbf{u} = 0$ given the eigenvalue λ . Another example is the computation of probability distribution in the overflow queuing problem [7, 8].

Now we assume the linear system

$$(2.12) \quad \mathbf{A}\mathbf{u} = 0$$

admits nontrivial solutions. If we solve (2.12) via the unconstrained optimization (2.10), common optimizers such as gradient descent will probably converge to zero due to the implicit regularization of NNs [5]. This issue can be solved by setting constraints on the solution. For example, we require $\|\mathbf{u}\|_p = 1$, then following (2.10) a penalized optimization for (2.12) is given by

$$(2.13) \quad \min_{\theta} L(\theta) := \frac{1}{N^d} \|\mathbf{A}\Phi(\theta)\|_2^2 + \varepsilon^{-1} (\|\Phi(\theta)\|_p - 1)^2,$$

where $\epsilon > 0$ is a penalty parameter.

A more simple way is fixing one component of \mathbf{u} , say $u_{j_1, \dots, j_d} = 1$ for some index (j_1, \dots, j_d) , if u_{j_1, \dots, j_d} is known to be nonzero in advance. In this case, the penalized optimization for (2.12) is as follows,

$$(2.14) \quad \min_{\theta} L(\theta) := \frac{1}{N^d} \|\mathbf{A}\Phi(\theta)\|_2^2 + \epsilon^{-1} (\phi(x_{j_1}, \dots, x_{j_d}; \theta) - 1)^2.$$

2.4. Stochastic gradient descent algorithm. Let us describe the practical algorithms using gradient descent for the optimization (2.10). The algorithms for optimization (2.13) and (2.14) computing nontrivial solutions can be derived in similar ways.

We rewrite \mathbf{A} and \mathbf{b} by blocks as follows

$$(2.15) \quad \mathbf{A} = [\mathbf{a}_1 \ \cdots \ \mathbf{a}_{N^d}]^\top, \quad \mathbf{b} = [b_1 \ \cdots \ b_{N^d}]^\top,$$

where $\mathbf{a} \in \mathbb{R}^{N^d}$ and $b_k \in \mathbb{R}$ for all k . Then the loss function L in (2.10) can be rewritten as

$$(2.16) \quad \min_{\theta} L(\theta) = \frac{1}{N^d} \sum_{k=1}^{N^d} |\mathbf{a}_k^\top \Phi(\theta) - b_k|^2.$$

To reduce L , a gradient descent scenario will update θ in every iteration by

$$(2.17) \quad \theta \leftarrow \theta - \tau \nabla_{\theta} L(\theta)$$

with

$$(2.18) \quad \nabla_{\theta} L(\theta) = \frac{2}{N^d} \sum_{k=1}^{N^d} \left(\mathbf{a}_k^\top \Phi(\theta) - b_k \right) \cdot \nabla_{\theta} \Phi(\theta)^\top \mathbf{a}_k,$$

where $\nabla_{\theta} \Phi(\theta)$ is the Jacobian matrix of Φ and $\tau > 0$ is some adaptive learning rate.

However, it is sometimes unavailable to add up all N^d terms in (2.18) due to the limit of computational resources. So in practice, one can use stochastic gradient descent by selecting a small training subset among all terms in every iteration. More precisely, θ is updated by

$$(2.19) \quad \theta \leftarrow \theta - \tau \nabla_{\theta} L_{\mathcal{S}}(\theta),$$

where $\mathcal{S} \subset \mathcal{I}_{N^d} := \{1, 2, \dots, N^d\}$ and

$$(2.20) \quad L_{\mathcal{S}}(\theta) = \frac{1}{|\mathcal{S}|} \sum_{k \in \mathcal{S}} |\mathbf{a}_k^\top \Phi(\theta) - b_k|^2,$$

$$(2.21) \quad \nabla_{\theta} L_{\mathcal{S}}(\theta) = \frac{2}{|\mathcal{S}|} \sum_{k \in \mathcal{S}} \left(\mathbf{a}_k^\top \Phi(\theta) - b_k \right) \cdot \nabla_{\theta} \Phi(\theta)^\top \mathbf{a}_k.$$

In each iteration, the training set \mathcal{S} will be selected from \mathcal{I}_{N^d} according to some principles. Summarily, we have Algorithm 1 using stochastic gradient descent.

In Algorithm 1, $\nabla_{\theta} L_{\mathcal{S}}(\theta)$ is computed with the formula (2.21). Algorithm 1 sets up a fundamental framework for the NN-based method to solve general linear systems. Compare to traditional iterative methods which rely on matrix-vector multiplications, Algorithm 1 requires extra cost to

Algorithm 1 NN-based stochastic gradient descent to solve linear systems

Input: data $\mathbf{A} \in \mathbb{R}^{N^d \times N^d}$, $\mathbf{b} \in \mathbb{R}^{N^d}$; hyper-parameters $L, M, \sigma, \{\tau_i\}$

Output: approximate solution $\mathbf{u}_{\text{appro}}$ of $\mathbf{A}\mathbf{u} = \mathbf{b}$.

initialize $\phi(x; \theta) \in \mathcal{F}_{L,M,\sigma}$ with $\theta \leftarrow \theta_0$

$i \leftarrow 1$

while stopping criteria is not satisfied **do**

 generate $\mathcal{S} \subset \mathcal{I}_{N^d}$

$\theta \leftarrow \theta - \tau_i \nabla_{\theta} L_{\mathcal{S}}(\theta)$

$i \leftarrow i + 1$

end while

$\mathbf{u}_{\text{appro}} \leftarrow \Phi(\theta)$

compute NN-related quantities $\Phi(\theta)$ and $\nabla_{\theta} L_{\mathcal{S}}(\theta)$. Hence, this method is not advantageous for general linear systems, especially those with small sizes.

However, this method is able to address very large-scale linear systems that traditional methods may not handle. Now let us assume \mathbf{A} is a sparse matrix with at most N_{nz} nonzero entries in each row. For some linear systems derived from high-dimensional physical problems, the size N^d is extremely large, and the available storage is not large enough to save the data \mathbf{A} or \mathbf{b} . In such cases, \mathbf{A} and \mathbf{b} are usually provided in the form of index functions. Specifically, define the function \hat{A} such that for all $k \in \mathcal{I}_{N^d}$,

$$(2.22) \quad \hat{A}(k) = \{(j, A_{kj}) : A_{kj} \neq 0\},$$

which is the set of all nonzero entries in the k -th row of \mathbf{A} . Similarly, define the function \hat{b} such that for all $k \in \mathcal{I}_{N^d}$,

$$(2.23) \quad \hat{b}(k) = b_k,$$

which is the k -th component of \mathbf{b} . In practice, \hat{A} and \hat{b} can be implemented as data loading or real-time computation.

Similarly, due to the limit of storage, it may not be allowed to save the intermediate solution vector $\Phi(\theta)$ in memory. But thanks to the smaller size of θ , we can always save θ and compute Φ at specified indices. This is a significant advantage over traditional methods that need to save the entire solution vector all the time. In the end, we output the approximate solution in the form of an index function $\hat{\phi}$, which is defined as

$$(2.24) \quad \hat{\phi}(k) = \Phi_k,$$

which is the k -th entry of Φ . To sum up, we improve Algorithm 1 to the memory-saving Algorithm 2 for large-scale linear systems. Here we use $\hat{x}(j)$ to denote the j -th grid point in the lexicographically ordered sequence of Γ .

The complexity of each iteration of the **while**-loop can be estimated. We ignore the complexity of calling index functions \hat{A} or \hat{b} since it is data loading and not involved by the method. By a simple calculation, we can derive that it costs $O(LM^2 + dM)$ to compute $\phi(x; \theta)$ and $\nabla_{\theta} \phi(x; \theta)$ at each point $x \in \mathbb{R}^d$, namely, doing forward and back propagation of NNs. So the total complexity of

Algorithm 2 NN-based stochastic gradient descent to solve linear systems (memory-saving)

Input: index functions \widehat{A}, \widehat{b} ; hyper parameters $L, M, \sigma, \{\tau_i\}$

Output: index function $\widehat{\phi}$ such that $\widehat{\phi}(j)$ approximates the j -th component of \mathbf{u} satisfying $\mathbf{A}\mathbf{u} = \mathbf{b}$

```

initialize  $\phi(x; \theta) \in \mathcal{F}_{L,M,\sigma}$  with  $\theta \leftarrow \theta_0$ 
 $i \leftarrow 1$ 
while stopping criteria is not satisfied do
  generate  $\mathcal{S} \subset \mathcal{I}_{N^d}$ 
   $g \leftarrow [0 \ \cdots \ 0]^\top \in \mathbb{R}^{|\theta|}$ 
  for  $k \in \mathcal{S}$  do
     $s_1 \leftarrow 0, s_2 \leftarrow [0 \ \cdots \ 0]^\top \in \mathbb{R}^{|\theta|}$ 
    for  $(j, A_{kj}) \in \widehat{A}(k)$  do
       $s_1 \leftarrow s_1 + A_{kj}\phi(\widehat{x}(j); \theta), s_2 \leftarrow s_2 + A_{kj}\nabla_\theta\phi(\widehat{x}(j); \theta)$ 
    end for
     $g \leftarrow g + (s_1 - \widehat{b}(k))s_2$ 
  end for
   $\theta \leftarrow \theta - \tau_i \cdot \frac{2}{|\mathcal{S}|}g$ 
   $i \leftarrow i + 1$ 
end while
 $\widehat{\phi}(j) := \phi(\widehat{x}(j); \theta)$ 

```

every iteration is $O(N_{\text{nz}}|\mathcal{S}|(LM^2 + dM))$. However, it is hard to estimate the number of iterations needed to satisfy the stopping criteria.

We remark that the proposed method is not limited to linear systems with tensor product structures. In Algorithm 1 and 2, the matrix \mathbf{A} and its index function \widehat{A} are general. We do not exploit any specialty of the matrix structure. This is essentially different from some existing methods for large-scale linear systems that rely on the matrix's special property.

3. Error analysis. We will give error analysis of the proposed method in this section. The method is developed based on the approximation property from NNs to smooth functions. Therefore, the analysis should depend on the regularity hypothesis of the target function v . Results of the NN approximation theory have been widely developed. Especially in this paper, we consider the NN approximation for Barron-type functions, which is studied extensively in [17, 13, 38, 39, 6, 15]. In these works, a significant fact is illustrated that the approximation error of two-layer FNNs for Barron-type functions is independent of the dimension or increases with it very slowly, hence overcoming the curse of dimensionality. Among various types of Barron spaces, we specifically use the definition described in [17], which corresponds to infinitely wide two-layer ReLU FNNs. Without loss of generality, it is still assumed that $\Omega = [0, 1]^d$ in the analysis.

As discussed in the Section 2.1, the class of two-layer (i.e., $L = 2$) FNNs can be reformulated as follows,

$$(3.1) \quad \mathcal{F}_{2,M,\text{ReLU}} = \left\{ \phi : \phi(x) = \frac{1}{M} \sum_{i=1}^M a_i \sigma(b_i^T x + c_i), \quad \forall (a_i, b_i, c_i) \in \mathbb{R} \times \mathbb{R}^d \times \mathbb{R} \right\}.$$

Let us introduce the Barron space and its norm with respect to $\mathcal{F}_{2,M,\text{ReLU}}$. Given a probability

measure π on $\mathbb{R} \times \mathbb{R}^d \times \mathbb{R}$, we set the function

$$(3.2) \quad f_\pi(x) = \int_{\mathcal{D}} a\sigma(b^T x + c)\pi(da, db, dc) = \mathbb{E}_\pi[a\sigma(b^T x + c)], \quad \forall x \in \mathbb{R}^d,$$

given this expression exists. For a function $v : \mathbb{R}^d \rightarrow \mathbb{R}$, we use Π_v to denote the set of all probability measures π such that $f_\pi(x) = v(x)$ almost everywhere. Then the Barron norm is defined as

$$(3.3) \quad \|v\|_{\mathcal{B}}^2 := \inf_{\pi \in \Pi_v} \int_{\mathbb{R} \times \mathbb{R}^d \times \mathbb{R}} a^2(|b| + |c|)^2 \pi(da, db, dc) = \inf_{\pi \in \Pi_v} \mathbb{E}_\pi[a^2(|b| + |c|)^2].$$

The infimum of the empty set is considered as $+\infty$. The set of all functions with finite Barron norm is denoted by \mathcal{B} . Note that \mathcal{B} equipped with the Barron norm is shown to be a Banach space that is named as Barron space [17].

The following result characterizes the approximation error of NNs in $\mathcal{F}_{2,M,\text{ReLU}}$ for functions in \mathcal{B} .

LEMMA 3.1 (Theorem 12, [13]). *For any $v \in \mathcal{B}$ and any $M \in \mathbb{N}^+$, there exists a two-layer ReLU FNN ϕ in $\mathcal{F}_{2,M,\text{ReLU}}$ such that*

$$(3.4) \quad \|v - \phi\|_{L^\infty([0,1]^d)} \leq 4\|v\|_{\mathcal{B}} \sqrt{\frac{d+1}{M}}.$$

On the other hand, it is naturally assumed that the linear system (2.6) is a good approximation to the original problem. More precisely, we formulate the following convergence assumption.

ASSUMPTION 3.1. *The solution \mathbf{u} of the linear system (2.6) satisfies*

$$(3.5) \quad |u_{i_1, \dots, i_d} - v(x_{i_1}, \dots, x_{i_d})| \leq \delta(N), \quad \forall (x_{i_1}, \dots, x_{i_d}) \in \Gamma,$$

for some $\delta(N) > 0$ and $\lim_{N \rightarrow \infty} \delta(N) = 0$.

Assumption 3.1 is often true in many applications. For example, Poisson's equation discretized by p -th order centered finite difference method with uniform grid spacing leads to $\delta(N) = CN^{-p}$ with some number $C > 0$ only depending on v [25]. We can view $\delta(N)$ as the discretization error between the linear system and the original continuous problem.

Now let us consider our method, i.e., the NN-based minimization (2.10). The following result shows that the error of our proposed method is bounded by the sum of the approximation error and the discretization error.

THEOREM 3.2. *Let θ^* be a minimizer of (2.10) with ϕ being an FNN of depth L and width M . Let \mathbf{u} be the solution of the linear system (2.6). Suppose that v is a function in \mathcal{B} . If Assumption 3.1 holds, it satisfies*

$$(3.6) \quad \|\Phi(\theta^*) - \mathbf{u}\|_\infty \leq \kappa(\mathbf{A}) \left(4\|v\|_{\mathcal{B}} \sqrt{\frac{d+1}{M}} + \delta(N) \right),$$

where $\kappa(\mathbf{A}) := \|\mathbf{A}\|_\infty \|\mathbf{A}^{-1}\|_\infty$ is the condition number of \mathbf{A} .

Proof. By Lemma 3.1, there exists some θ' such that $\phi(x; \theta')$ satisfies (3.4) for all $x \in \Omega$. Denote

$$(3.7) \quad \mathbf{v} := [v(x_1, \dots, x_1) \ v(x_1, \dots, x_2) \ \cdots \ v(x_N, \dots, x_N)]^\top,$$

it follows that

$$\begin{aligned}
 (3.8) \quad \|\Phi(\theta^*) - \mathbf{u}\|_\infty &\leq \|\mathbf{A}^{-1}\|_\infty \|\mathbf{A}\Phi(\theta^*) - \mathbf{b}\|_\infty \leq \|\mathbf{A}^{-1}\|_\infty \|\mathbf{A}\Phi(\theta') - \mathbf{b}\|_\infty \\
 &\leq \|\mathbf{A}^{-1}\|_\infty \|\mathbf{A}\Phi(\theta') - \mathbf{A}\mathbf{u}\|_\infty \leq \kappa(\mathbf{A}) \|\Phi(\theta') - \mathbf{u}\|_\infty \leq \kappa(\mathbf{A}) (\|\Phi(\theta') - \mathbf{v}\|_\infty + \|\mathbf{v} - \mathbf{u}\|_\infty) \\
 &\leq \kappa(\mathbf{A}) \left(4\|v\|_{\mathcal{B}} \sqrt{\frac{d+1}{M}} + \delta(N) \right).
 \end{aligned}$$

□

4. Numerical experiments. In this section, several linear systems from physically relevant problems are solved by the proposed NN-based method. Due to the high nonlinearity of NNs concerning their parameters, the least-squares optimization in this method is very nonlinear and, hence, difficult to solve. In practice, we can only find local minimizers rather than global minimizers, which causes a certain amount of optimization error. The optimization error then limits the accuracy of the numerical solution. Consequently, for small linear systems, our NN-based method performs less accurately than well-developed traditional methods (e.g., conjugate gradient method and GMRES), which can achieve errors around machine precision for well-conditioned systems. Nevertheless, this method is capable of extremely large linear systems that traditional methods cannot deal with. In this paper, we choose extremely large systems as numerical examples that are exclusively solved by our method, and we do not have any comparison tests.

The overall setting of implementation is summarized as follows.

- *Environment.* The method is tested in Python environment. PyTorch library with CUDA toolkit is utilized for neural network implementation and GPU-based parallel computing.
- *Optimizer and hyper-parameters.* The Algorithm 2 using stochastic gradient descent is implemented. In each iteration, we randomly select a batch of grid points from Γ with uniform distribution and take their indices to form \mathcal{S} . The learning rates are set to decay from 10^{-3} to 10^{-5} for all examples.
- *Network setting.* FNNs with ReLU activation functions are used in the experiments. We implement the method with various depth L and width M to investigate their effects. The network parameters are initialized by

$$(4.1) \quad a, W_l, b_l \sim U(-\sqrt{M}, \sqrt{M}), \quad l = 1, \dots, L.$$

- *Testing set and error evaluation.* We prescribe a set of N_{test} grid points from Γ with uniform distribution and take their indices as the testing set, denoted as $\mathcal{T} := \{(i_1^n, \dots, i_d^n)\}_{n=1}^{N_{\text{test}}}$. For the examples given true solutions, we compute the following ∞ -error over \mathcal{T}

$$(4.2) \quad e_\infty(\mathcal{T}) := \max_{(i_1^n, \dots, i_d^n) \in \mathcal{T}} |u_{i_1^n, \dots, i_d^n} - \phi(x_{i_1^n}, \dots, x_{i_d^n}; \theta)|.$$

and ℓ^2 -error over \mathcal{T} ,

$$(4.3) \quad e_{\ell^2}(\mathcal{T}) := \left(N_{\text{test}}^{-1} \sum_{(i_1^n, \dots, i_d^n) \in \mathcal{T}} |u_{i_1^n, \dots, i_d^n} - \phi(x_{i_1^n}, \dots, x_{i_d^n}; \theta)|^2 \right)^{\frac{1}{2}}.$$

And for the examples whose true solutions are unknown, we compute the following ℓ^2 -residual over \mathcal{T}

$$(4.4) \quad \begin{aligned} \text{Res}_{\ell^2}(\mathcal{T}) &:= \left(N_{\text{test}}^{-1} \sum_{(i_1^n, \dots, i_d^n) \in \mathcal{T}} [\mathbf{b} - \mathbf{A}\Phi(\theta)]_{\zeta(n)}^2 \right)^{\frac{1}{2}} \\ &= \left(N_{\text{test}}^{-1} \sum_{(i_1^n, \dots, i_d^n) \in \mathcal{T}} |b_{\zeta(n)} - \mathbf{a}_{\zeta(n)}^\top \Phi(\theta)|^2 \right)^{\frac{1}{2}}, \end{aligned}$$

where $\zeta(n) = \sum_{k=1}^d (i_k^n - 1)N^{d-k} + 1$ is the position of the index (i_1^n, \dots, i_d^n) in the lexicographical sequence. In all examples, N_{test} is set as 10^4 .

4.1. Poisson's equation. We consider the Poisson's equation

$$(4.5) \quad \begin{cases} -\Delta v(x) = f(x), & \text{in } \Omega := [-1, 1]^d, \\ v(x) = 0, & \text{on } \partial\Omega, \end{cases}$$

which is an elliptic partial differential equation describing a variety of steady-state physical phenomena. A widely used approach for (4.5) is the second-order centered finite difference scheme with uniform grid spacing, which leads to the following matrix,

$$(4.6) \quad \mathbf{A} = \sum_{n=1}^d \underbrace{\mathbf{I}_N \otimes \dots \otimes \mathbf{I}_N}_{n-1 \text{ terms}} \otimes \mathbf{T} \otimes \underbrace{\mathbf{I}_N \otimes \dots \otimes \mathbf{I}_N}_{d-n \text{ terms}},$$

where \otimes denotes the Kronecker product; $\mathbf{I}_N \in \mathbb{R}^{N \times N}$ is the identity matrix; $\mathbf{T} = [T_{i,j}] \in \mathbb{R}^{N \times N}$ is given by

$$(4.7) \quad T_{i,j} = \begin{cases} -2/h^2, & j = i, \\ 1/h^2, & j = i \pm 1, \\ 0, & \text{else;} \end{cases}$$

$h = 2/(N+1)$ is the grid size. We set the physical solution of (4.6) as

$$(4.8) \quad v(x) = \prod_{i=1}^d \sin(\pi x_i).$$

To compute the error accurately, we artificially set the true solution of the linear system. In this experiment, we simply set $\mathbf{u}_{\text{true}} = \mathbf{v}$ (defined in (3.7)) as the true solution. Namely, we ignore the discretization error and directly take the physical solution as the solution of the linear system. The right hand side is thereafter computed as $\mathbf{b} = \mathbf{A}\mathbf{u}_{\text{true}}$.

We solve $\mathbf{A}\mathbf{u} = \mathbf{b}$ for $d = 3, 6$ using Algorithm 2, in which we input the matrix index function \hat{A} and the right hand side index function \hat{b} extracted from \mathbf{A} and \mathbf{b} , respectively. The experiment is repeated for various N and FNN sizes (L, M) . The batch size $|\mathcal{S}|$ is set as 10^4 , and the number of iterations is fixed as 5×10^4 . The results are shown in Table 4.1. It is observed that the error is

reduced as L or M increases but keeps almost unchanged for various N . This is reasonable since the discretization error $\delta(N)$ vanishes in our setting and the final error only depends on the size of the used FNN.

Moreover, the number of unknown parameters $|\theta|$ is at most 41200 ($L = 3, M = 200$), which is much less than N^d , the size of the linear system. Specifically, in the case $d = 6$ and $N = 10^4$, the size $N^d = 10^{24}$ is extremely large¹ that prevents one using traditional linear solvers, yet the proposed NN-based method is still effective, obtaining ∞ -errors at best $O(10^{-3})$.

We also present the error curve versus iterations in Figure 4.1 to visualize the dynamics of the optimization. It is observed the error decreases rapidly in the first few iterations and decreases slowly afterward. This means a rough solution can be obtained within much fewer iterations.

	$d = 3$			$d = 6$		
	$N = 10^2$	$N = 10^3$	$N = 10^4$	$N = 10^2$	$N = 10^3$	$N = 10^4$
$L = 2, M = 100$ ($ \theta = 500$)	4.820e-03	5.056e-03	4.915e-03	1.694e-01	1.795e-01	1.646e-01
$L = 2, M = 200$ ($ \theta = 1000$)	2.245e-03	2.209e-03	2.044e-03	4.989e-02	5.106e-02	4.969e-02
$L = 3, M = 100$ ($ \theta = 10600$)	2.695e-04	2.707e-04	2.591e-04	1.368e-02	1.447e-02	1.377e-02
$L = 3, M = 200$ ($ \theta = 41200$)	1.846e-04	2.027e-04	1.953e-04	4.916e-03	4.435e-03	4.531e-03

(a) ∞ -error

	$d = 3$			$d = 6$		
	$N = 10^2$	$N = 10^3$	$N = 10^4$	$N = 10^2$	$N = 10^3$	$N = 10^4$
$L = 2, M = 100$ ($ \theta = 500$)	1.036e-03	1.067e-03	1.042e-03	1.739e-02	1.738e-02	1.670e-02
$L = 2, M = 200$ ($ \theta = 1000$)	3.774e-04	3.632e-04	3.594e-04	7.295e-03	7.326e-03	7.322e-03
$L = 3, M = 100$ ($ \theta = 10600$)	6.878e-05	6.897e-05	6.688e-05	2.145e-03	2.125e-03	2.109e-03
$L = 3, M = 200$ ($ \theta = 41200$)	5.412e-05	5.901e-05	5.745e-05	7.950e-04	7.577e-04	7.627e-04

(b) ℓ^2 -errorTable 4.1: *Solution errors of the Poisson's equation for various d, N, L and M .*

4.2. Riesz fractional diffusion. Let us consider the following Riesz fractional diffusion equation,

$$(4.9) \quad - \sum_{n=1}^d c_n \frac{\partial^{\alpha_n} v}{\partial |x_n|^{\alpha_n}} = y(x), \quad \text{in } \Omega := [-1, 1]^d$$

¹The ratio of $41200/10^{24}$ is about $4\text{e-}20$.

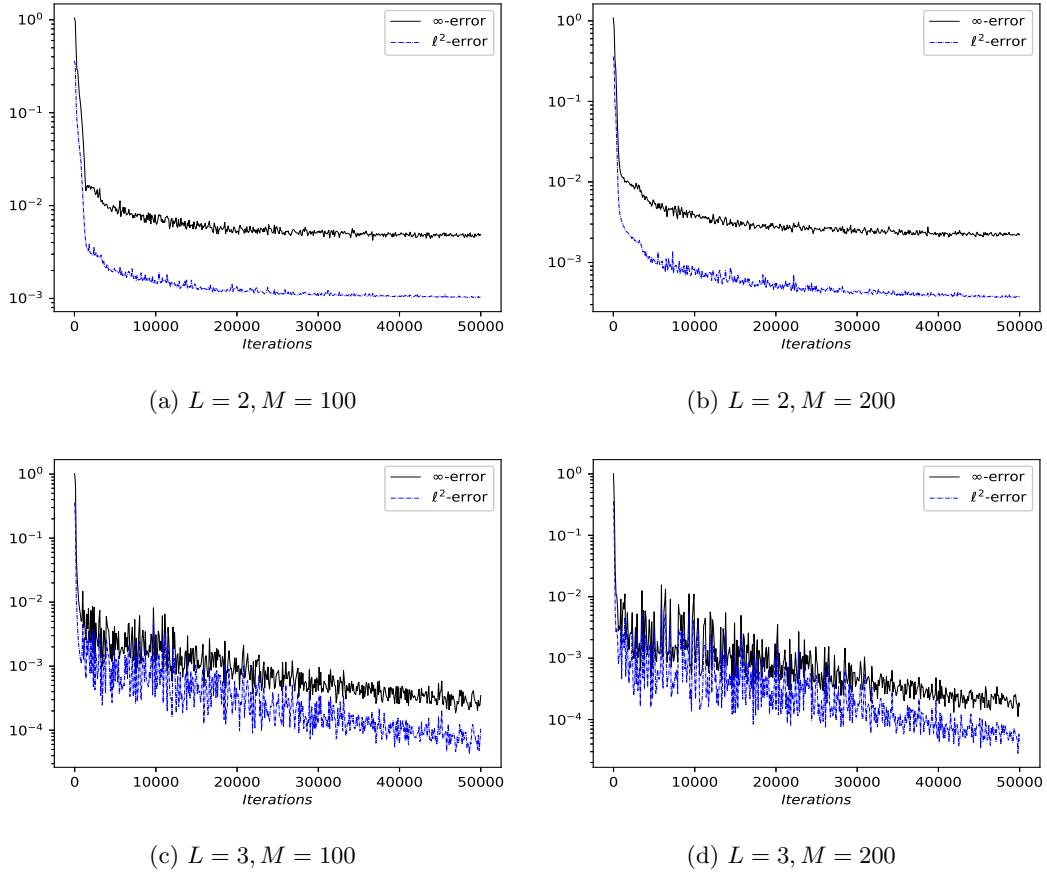


Fig. 4.1: Errors versus iterations for various FNN sizes in the Poisson's equation ($d = 3$).

where $c_n > 0, 1 < \alpha_n < 2$ for all n and $\frac{\partial^{\alpha_n} v}{\partial |x_n|^{\alpha_n}}$ is the Riesz fractional derivative (see [21]). Employing finite difference method on (4.9) leads to a linear system whose matrix \mathbf{A} is given by

$$(4.10) \quad \mathbf{A} = \sum_{n=1}^d \underbrace{\mathbf{I}_N \otimes \cdots \otimes \mathbf{I}_N}_{n-1 \text{ terms}} \otimes \mathbf{T}^{(n)} \otimes \underbrace{\mathbf{I}_N \otimes \cdots \otimes \mathbf{I}_N}_{d-n \text{ terms}},$$

with $\mathbf{T}^{(n)}$ being the Toeplitz matrix

$$(4.11) \quad \mathbf{T}^{(n)} := \begin{bmatrix} 2t_1^{(n)} & t_0^{(n)} + t_2^{(n)} & t_3^{(n)} & \cdots & t_{N-1}^{(n)} & t_N^{(n)} \\ t_0^{(n)} + t_2^{(n)} & 2t_1^{(n)} & t_0^{(n)} + t_2^{(n)} & t_3^{(n)} & \cdots & t_{N-1}^{(n)} \\ \vdots & t_0^{(n)} + t_2^{(n)} & 2t_1^{(n)} & \cdots & \cdots & \vdots \\ \vdots & \cdots & \cdots & \cdots & \cdots & t_3^{(n)} \\ t_{N-1}^{(n)} & \cdots & \cdots & \cdots & 2t_1^{(n)} & t_0^{(n)} + t_2^{(n)} \\ t_N^{(n)} & t_{N-1}^{(n)} & \cdots & \cdots & t_0^{(n)} + t_2^{(n)} & 2t_1^{(n)} \end{bmatrix} \in \mathbb{R}^{N \times N},$$

and $t_0^{(n)} := \frac{c_n}{2 \cos(\frac{\alpha_n \pi}{2}) h^{\alpha_n}}$, $t_i^{(n)} = (1 - \frac{\alpha_n + 1}{i}) t_{i-1}^{(n)}$ for $1 \leq i \leq N$. The matrix \mathbf{A} is ill-conditioned, and some preconditioning techniques have been developed (e.g., [28, 12, 30, 11, 21]). In prior work, the linear system with at most $d = 3$ is solved.

In this experiment, we set $c_n = 1$ and $\alpha_n = 1.5$ for all n . We solve $\mathbf{A}\mathbf{u} = \mathbf{b}$ for $d = 5, 10$ and $N = 10$ using Algorithm 2, where the true solution is set as $\mathbf{u}_{\text{true}} = \mathbf{v}$ with $v(x) = \sin(\sum_{n=1}^d x_n)$. We set $|\mathcal{S}| = 2 \times 10^4$ and the number of iteration to be 2×10^4 . Results are shown in Table 4.2. It is clear that the deeper networks with $L = 3$ outperform the shallow ones with $L = 2$ in general. However, in the case $d = 10$, the wide network with $(L, M) = (3, 200)$ perform worse than the narrow one with $(L, M) = (3, 100)$. It implies that larger networks are sometimes more difficult to train than smaller ones, resulting in more significant optimization errors. Despite being more accurate in approximation, larger networks may not provide better numerical results in practice.

	$d = 5$		$d = 10$	
	∞ -error	ℓ^2 -error	∞ -error	ℓ^2 -error
$L = 2, M = 100$ ($ \theta = 500$)	8.341e-01	3.674e-02	9.953e-02	7.481e-03
$L = 2, M = 200$ ($ \theta = 1000$)	4.254e-01	1.455e-02	9.659e-02	7.128e-03
$L = 3, M = 100$ ($ \theta = 10600$)	5.820e-03	6.162e-04	2.272e-02	7.976e-04
$L = 3, M = 200$ ($ \theta = 41200$)	2.078e-03	4.662e-04	2.931e-02	1.483e-03

Table 4.2: *Solution errors of the Riesz fractional diffusion for various d , L and M .*

4.3. Overflow queuing model. The next example is the overflow queuing model proposed in [7, 8]. Suppose there are d queues with individual queue size N , one aims to find nontrivial solutions of the following $N^d \times N^d$ linear system,

$$(4.12) \quad (\mathbf{A} + \mathbf{R})\mathbf{u} = 0.$$

Here the first part \mathbf{A} has the tensor product structure (4.10) with

$$\mathbf{T}^{(n)} := \begin{bmatrix} \lambda_n & -\mu_n & & & & \\ -\lambda_n & \lambda_n + \mu_n & -2\mu_n & & & \\ & -\lambda_n & \lambda_n + 2\mu_n & -3\mu_n & & \\ & & \ddots & \ddots & \ddots & \\ & & & -\lambda_n & \lambda_n + s_n \mu_n & -s_n \mu_n \\ & & & & \ddots & \ddots & \ddots \\ & & & & & -\lambda_n & \lambda_n + s_n \mu_n & -s_n \mu_n \\ & & & & & & -\lambda_n & s_n \mu_n \end{bmatrix} \in \mathbb{R}^{N \times N},$$

where $s_n \in \mathbb{N}^+$, $\lambda_n, \alpha \in \mathbb{R}^+$ are physically relevant parameters, and $\mu_n := s_n^{-1}(\lambda_n + (N - 1)^{-\alpha})$. The second part $\mathbf{R} = \sum_{m \neq n} \mathbf{R}_{mn}$ with

$$(4.13) \quad \mathbf{R}_{mn} = \bigotimes_{k=1}^d (e_m e_m^\top)^{\delta_{mk}} \mathbf{R}_m^{\delta_{nk}},$$

where e_m is the m -th unit vector in \mathbb{R}^N , δ_{mn} is the Kronecker delta, and

$$(4.14) \quad \mathbf{R}_m := \lambda_m \begin{bmatrix} 1 & & & & \\ -1 & 1 & & & \\ & & \ddots & \ddots & \\ & & & -1 & 1 \\ & & & & -1 & 0 \end{bmatrix}.$$

The (normalized) nontrivial solution \mathbf{u} represents the steady-state probability distribution of the queue system. More precisely, u_{i_1, i_2, \dots, i_d} is the probability that i_k customers are in the k -th queue for $k = 1, \dots, d$. One can show that $\mathbf{A} + \mathbf{R}$ has a one-dimensional null-space. In prior work, one at most solves the linear system with $d = 2$.

We use the least-squares model with penalty (2.14) to solve (4.12) for $d = 5, 10$, in which the first component of \mathbf{u} is fixed as 1 and the penalty parameter ε is set as 1.0. Since the original problem does not involve any physical domains, a fictitious domain $[0, 1]^d$ is introduced for the implementation. We set $N = 100$, $\alpha = 1$, $\lambda_n = 0.01$ and $s_n = 8n$ for $n = 1, \dots, d$. The algorithm is implemented with $|\mathcal{S}| = 2 \times 10^4$ and number of iterations being 2×10^4 . The residuals of the obtained solutions are listed in Table 4.3.

We are also interested in the landscape of the solution. Specifically, in the case $d = 10$, $L = 2$ and $M = 200$, we find $x_{\max} = x_{2,6,10,15,18,24,27,32,36,40}$ is the location where the approximate solution $\Phi(\theta)$ takes its maximum 2.155. It is intuitive to find that the n -th index of x_{\max} is equal or close to $s_n/2$. To show a more clear distribution of the solution, we present the 2-D slices passing through x_{\max} in Figure 4.2.

	$d = 5$	$d = 10$
$L = 2, M = 100$ ($ \theta = 500$)	7.544e-04	1.183e-03
$L = 2, M = 200$ ($ \theta = 1000$)	7.328e-04	1.193e-03
$L = 3, M = 100$ ($ \theta = 10600$)	6.629e-04	1.087e-03
$L = 3, M = 200$ ($ \theta = 41200$)	6.733e-04	1.052e-03

Table 4.3: *Residuals of the queuing problem for various d , L and M .*

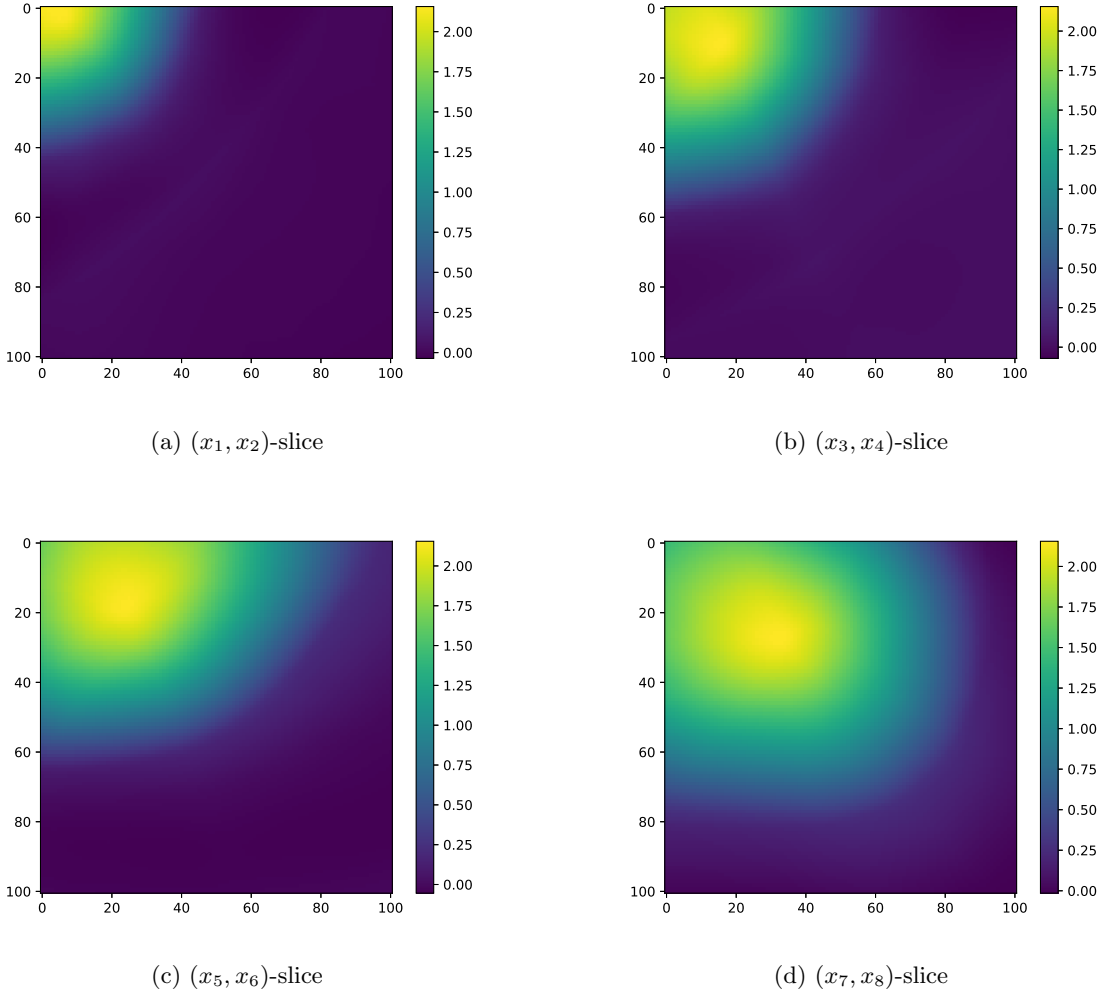


Fig. 4.2: 2-D slices of the numerical solution $\phi(x, \theta)$ passing through the maximal point x_{\max} in the queuing problem ($d = 10, L = 3, M = 200$).

4.4. Probabilistic Boolean networks. Let us consider the steady-state probability distribution of probabilistic Boolean networks, which are widely applied in real-world problems such as genomic signal processing [26]. In this problem, one aims to find the eigenvector associated with the principle eigenvalue 1 of the transition probability matrix, and the normalized eigenvector exactly represents the steady-state probability distribution. The transition probability matrix is of size 2^d by 2^d , where d is the number of genes.

In our experiment, we generate a sparse Toeplitz matrix $\tilde{\mathbf{T}} = [t_{ij}] \in \mathbb{R}^{2^d \times 2^d}$ by

$$(4.15) \quad t_{ij} = \begin{cases} v_k, & \text{if } j = i + k \text{ for some } k \in \mathcal{I}, \\ 0, & \text{otherwise,} \end{cases}$$

where \mathcal{I} is a prescribed sparse subset of $\{-2^d, -2^d + 1, \dots, 2^d\}$ and $\{v_k\}_{k \in \mathcal{I}}$ is a prescribed set of positive constants. Followed by column normalization on $\tilde{\mathbf{T}}$, we obtain the transition probability matrix \mathbf{T} whose each column adds up to 1. In practice, we casually choose $\mathcal{I} = \{-13, -5, 2, 6\}$ and $\{v_{13}, v_{-5}, v_2, v_6\} = \{1, 4, 3, 2\}$.

The proposed method is implemented to find the principle eigenvector of \mathbf{T} . First, we introduce the fictitious domain $[0, 1]^d$ and take two grid points $1/3$ and $2/3$ in each dimension. Then we take the following penalized model to compute $(\mathbf{I} - \mathbf{T})\mathbf{u} = 0$,

$$(4.16) \quad \min_{\theta} \frac{1}{N^d} \|(\mathbf{I} - \mathbf{T})\Phi(\theta)\|_2^2 + \varepsilon^{-1} \left(N^{-d} \cdot \mathbf{1}^\top \Phi(\theta) - 1 \right)^2,$$

where $\mathbf{1}$ is the all-ones column vector in \mathbb{R}^{2^d} ; namely, we require the mean of the approximate solution to be 1. The model (4.16) is implemented using a stochastic gradient descent algorithm with $\varepsilon = 1.0$, $|\mathcal{S}| = 2 \times 10^4$ and number of iteration 2×10^4 . In each iteration, the term $N^{-d} \cdot \mathbf{1}^\top \Phi(\theta)$ is only calculated at the training points; specifically, we calculate $|\mathcal{S}|^{-1} \sum_{x \in \mathcal{S}} \phi(x; \theta)$ instead. The cases $d = 50$ and 100 are tested, where the matrix $\mathbf{I} - \mathbf{T}$ has $O(10^{15})$ and $O(10^{30})$ nonzero entries, respectively. The resulting residuals are listed in Table 4.4. We remark that our experiment computes much larger systems than the previous work [26], which solves the same problem with at most 30 dimensions and 5×10^4 nonzero entries.

	$d = 50$	$d = 100$
$L = 2, M = 100$ ($ \theta = 500$)	6.737e-04	1.755e-02
$L = 2, M = 200$ ($ \theta = 1000$)	6.230e-04	1.942e-02
$L = 3, M = 100$ ($ \theta = 10600$)	4.987e-04	3.616e-03
$L = 3, M = 200$ ($ \theta = 41200$)	6.466e-04	3.807e-03

Table 4.4: *Residuals of the probabilistic Boolean network problem for various d , L and M .*

5. Conclusion. This work develops a novel NN-based method for extremely large linear systems. The main advantage lies in the saving of storage. Specifically, we create a neural network representation for the unknown vector, containing much fewer unknowns than the original linear system. The system is then modified to a nonlinear least-squares optimization, and it can be solved by gradient descent under a deep learning framework. The proposed method allows us to deal with problems out of storage if using traditional linear solvers. Error estimate is also provided using the approximation property of NNs.

Several physically relevant problems are considered in the numerical experiments. This method is successfully implemented to solve the corresponding linear systems. Compared with prior work on these problems, we solve the systems of much larger sizes, usually intractable for other existing methods. However, the accuracy of this NN-based method is generally not as high as traditional ones due to the optimization error. Hence it is not recommended for small linear systems.

One direction of future work could be the convergence analysis of the gradient descent in solving the least-squares optimization. Namely, we could investigate whether the gradient descent

necessarily finds good minimizers. In recent years, some research work has been conducted on the convergence of gradient descent in neural network regression, yet it is significantly different from this situation. On the one hand, the loss function in this method is the residual of the linear system rather than the simple ℓ^2 or entropy loss discussed in prior work. On the other hand, most of the previous analysis is based on the over-parametrization hypothesis, in which the NN has much more parameters than terms in the loss function. But in this method, we expect to use NNs with much fewer parameters than equations or unknowns to save the storage.

We are also inspired by the last numerical example, in which the solution represents binary probability distribution and does not characterize any smooth physical quantities. One open question is whether the smoothness hypothesis of the solution is necessary for the success of this method if we regard the linear system as a $2^d \times 2^d$ structure. In this case, the approximate network only has to fit two points in every dimension. It is simply required that the network acts as a straight line in any dimension. Therefore it is interesting to investigate whether general $2^d \times 2^d$ linear systems can be handled by this method without many hypotheses on the solution.

REFERENCES

- [1] Z.-Z. Bai. Motivations and realizations of Krylov subspace methods for large sparse linear systems. *Journal of Computational and Applied Mathematics*, 283:71–78, 2015.
- [2] J. Ballani and L. Grasedyck. A projection method to solve linear systems in tensor format. *Numerical Linear Algebra with Applications*, 20:27–43, 2013.
- [3] A. R. Barron. Neural net approximation. In *Proceedings of the 7th Yale Workshop on Adaptive and Learning Systems*, 1992.
- [4] A. R. Barron. Universal approximation bounds for superpositions of a sigmoidal function. *IEEE Trans. Inform. Theory*, 39(3):930–945, 1993.
- [5] Y. Cao, Z. Fang, Y. Wu, D. X. Zhou, and Q. Gu. Towards understanding the spectral bias of deep learning. In *Proceedings of the Thirtieth International Joint Conference on Artificial Intelligence*, 2021.
- [6] A. Caragea, P. Petersen, and F. Voigtlaender. Neural network approximation and estimation of classifiers with classification boundary in a Barron class. *arXiv e-prints*, arXiv:2011.09363, 2020.
- [7] R. H. Chan. Iterative methods for overflow queueing models I. *Numerische Mathematik*, 51:143–180, 1987.
- [8] R. H. Chan. Iterative methods for overflow queueing models II. *Numerische Mathematik*, 54:57–78, 1988.
- [9] R. H. Chan and M. K. Ng. Conjugate gradient methods for Toeplitz systems. *SIAM Review*, 38:427–482, 1996.
- [10] G. Cybenko. Approximation by superpositions of a sigmoidal function. *Mathematics of Control, Signals and Systems*, 2(4):303–314, 1989.
- [11] M. Donatelli, R. Krause, M. Mazza, and K. Trotti. Multigrid preconditioners for anisotropic space-fractional diffusion equations. *Advances in Computational Mathematics*, 46, 2020.
- [12] M. Donatelli, M. Mazza, and S. Serra-Capizzano. Spectral analysis and structure preserving preconditioners for fractional diffusion equations. *Journal of Computational Physics*, 307:262–279, 2016.
- [13] W. E, C. Ma, S. Wojtowytsch, and L. Wu. Towards a mathematical understanding of neural network-based machine learning: what we know and what we don’t. *arXiv e-prints*, arXiv:2009.10713, 2020.
- [14] W. E, C. Ma, and L. Wu. A priori estimates of the population risk for two-layer neural networks. *Communications in Mathematical Sciences*, 17(5):1407–1425, 2019.
- [15] W. E, C. Ma, and L. Wu. The Barron space and the flow-induced function spaces for neural network models. *Constructive Approximation*, 55:369–406, 2022.
- [16] W. E and Q. Wang. Exponential convergence of the deep neural network approximation for analytic functions. *Science China Mathematics*, 61:1733–1740, 2018.
- [17] W. E and S. Wojtowytsch. Representation formulas and pointwise properties for Barron functions. *arXiv e-prints*, arXiv:2006.05982, 2020.
- [18] H.-Y. Fan, L. Zhang, E.-K. Chu, and Y. Wei. Numerical solution to a linear equation with tensor product structure. *Numerical Linear Algebra with Applications*, 24:e2106, 2017.
- [19] J. Han, A. Jentzen, and W. E. Solving high-dimensional partial differential equations using deep learning. *Proceedings of the National Academy of Sciences*, 115(34):8505–8510, 2018.

- [20] K. Hornik, M. Stinchcombe, and H. White. Multilayer feedforward networks are universal approximators. *Neural Networks*, 2(5):359–366, 1989.
- [21] X. Huang, X.-L. Lin, M. K. Ng, and H.-W. Sun. Spectral analysis for preconditioning of multi-dimensional Riesz fractional diffusion equations. *arXiv e-prints*, arXiv:2102.01371, 2021.
- [22] R. Keller and Q. Du. Discovery of dynamics using linear multistep methods. *SIAM Journal on Numerical Analysis*, 59:429–455, 2021.
- [23] J. M. Klusowski and A. R. Barron. Approximation by combinations of ReLU and squared ReLU ridge functions with ℓ^1 and ℓ^0 controls. *IEEE Trans. Inform. Theory*, 64(12):7649–7656, 2018.
- [24] D. Kressner and C. Tobler. Krylov subspace methods for linear systems with tensor product structure. *SIAM Journal on Matrix Analysis and Applications*, 31:1688–1714, 2010.
- [25] S. Larsson and V. Thomée. *Partial differential equations with numerical methods*. Springer, 2003.
- [26] W. Li, L.-B. Cui, and M. K. Ng. On computation of the steady-state probability distribution of probabilistic boolean networks with gene perturbation. *Journal of Computational and Applied Mathematics*, 236:4067–4081, 2012.
- [27] S. Liang and R. Srikant. Why deep neural networks for function approximation? In *International Conference on Learning Representations*, 2017.
- [28] F.-R. Lin and X.-Q. Jin S.-W. Yang. Preconditioned iterative methods for fractional diffusion equation. *Journal of Computational Physics*, 256:109–117, 2014.
- [29] Z. Lu, H. Pu, F. Wang, Z. Hu, and L. Wang. The expressive power of neural networks: A view from the width. In *Advances in Neural Information Processing Systems 30*, pages 6231–6239. Curran Associates, Inc., 2017.
- [30] H. Moghaderi, M. Dehghan, and M. Donatelli. Spectral analysis and multigrid preconditioners for two-dimensional space-fractional diffusion equations. *Journal of Computational Physics*, 350:992–1011, 2017.
- [31] H. Montanelli and Q. Du. New error bounds for deep ReLU networks using sparse grids. *SIAM Journal on Mathematics of Data Science*, 1:78–92, 2019.
- [32] H. Montanelli, H. Yang, and Q. Du. Deep ReLU networks overcome the curse of dimensionality for bandlimited functions. *Journal of Computational Mathematics*, 39:801–815, 2021.
- [33] Y.-Q. Niu and B. Zheng. A greedy block kaczmarz algorithm for solving large-scale linear systems. *Applied Mathematics Letters*, 104:106294, 2020.
- [34] P. Petersen and F. Voigtlaender. Optimal approximation of piecewise smooth functions using deep ReLU neural networks. *Neural Networks*, 108:296–330, 2018.
- [35] M. Raissi, P. Perdikaris, and G. E. Karniadakis. Physics-informed neural networks: A deep learning framework for solving forward and inverse problems involving nonlinear partial differential equations. *Journal of Computational Physics*, 378:686–707, 2019.
- [36] Z. Shen, H. Yang, and S. Zhang. Nonlinear approximation via compositions. *Neural Networks*, 119:74–84, 2019.
- [37] Z. Shen, H. Yang, and S. Zhang. Deep network approximation characterized by number of neurons. *Communications in Computational Physics*, 28(5):1768–1811, 2020.
- [38] J. W. Siegel and J. Xu. Approximation rates for neural networks with general activation functions. *Neural Networks*, 128:313–321, 2020.
- [39] J. W. Siegel and J. Xu. High-order approximation rates for neural networks with ReLU^k activation functions. *arXiv e-prints*, arXiv:2012.07205, 2020.
- [40] T. Suzuki. Adaptivity of deep ReLU network for learning in Besov and mixed smooth Besov spaces: optimal rate and curse of dimensionality. In *International Conference on Learning Representations*, 2018.
- [41] R. Tipireddy, P. Perdikaris, P. Stinis, and A. Tartakovsky. A comparative study of physics-informed neural network models for learning unknown dynamics and constitutive relations. *arXiv e-prints*, arXiv:1904.04058, 2019.
- [42] D. Yarotsky. Error bounds for approximations with deep ReLU networks. *Neural Networks*, 94:103–114, 2017.
- [43] D. Yarotsky. Optimal approximation of continuous functions by very deep ReLU networks. In *Conference on learning theory*, 2018.
- [44] Y. Zang, G. Bao, X. Ye, and H. Zhou. Weak adversarial networks for high-dimensional partial differential equations. *Journal of Computational Physics*, 411:109409, 2020.
- [45] J.-J. Zhang. A new greedy Kaczmarz algorithm for the solution of very large linear systems. *Applied Mathematics Letters*, 91:207–212, 2019.